Available online at www.sciencedirect.com

ScienceDirect

Geochimica et Cosmochimica Acta 280 (2020) 360–377

Geochimica et Cosmochimica Acta

www.elsevier.com/locate/gca

Cycling phosphorus on the Archean Earth: Part II. Phosphorus limitation on primary production in Archean ecosystems

Jihua Hao [a,b,*], Andrew H. Knoll [c], Fang Huang [d,e], Juergen Schieber [f], Robert M. Hazen [g], Isabelle Daniel [a]

[a] *Univ Lyon, Université Lyon 1, Ens de Lyon, CNRS, UMR 5276 LGL-TPE, F-69622 Villeurbanne, France*
[b] *Department of Marine and Coastal Sciences, Rutgers University, New Brunswick, NJ, 08901, USA*
[c] *Department of Organismic and Evolutionary Biology, Harvard University, Cambridge, MA 02138, USA*
[d] *Tetherless World Constellation, Rensselaer Polytechnic Institute, Troy, NY 12180, USA*
[e] *CSIRO Mineral Resources, Kensington, WA 6151, Australia*
[f] *Department of Earth and Atmospheric Sciences, Indiana University, Bloomington, IN 47405, USA*
[g] *Geophysical Laboratory, Carnegie Institution for Science, Washington DC 20015, USA*

Received 8 August 2019; accepted in revised form 3 April 2020; available online 15 April 2020

Abstract

Several lines of evidence point to low rates of net primary production (NPP) in Archean oceans. However, whether Archean NPP was limited by electron donors or nutrients, particularly phosphorus (P), and how these factors might have changed over a billion years of recorded Archean history, remains contentious. One major challenge is to understand quantitatively the biogeochemical cycling of P on the early Earth. In Part I of this series (Hao et al., 2020), we estimated the weathering flux of P to the oceans as a function of temporally increasing continental emergence and elevation through Archean time. In Part II, we conduct thermodynamic and kinetic simulations to understand key processes of P cycling within the Archean ocean, including seafloor weathering, recycling of organic P, the solubility and precipitation of secondary phosphate minerals, and the burial diagenesis of P precipitates. Our calculations suggest low solubilities of apatite minerals in Archean seawater, primarily due to nearly neutral pH and high levels of Ca. This low solubility, in turn, implies a negligible contribution of apatite dissolution to P bioavailability in Archean seawater.

We also simulate the solubility limits of common secondary P-bearing minerals, showing that vivianite would have been the least soluble P mineral in ferruginous Archean seawater (0.1–0.3 μM), even at moderate supersaturation states ($\Omega = 100$ or 1000). If vivianite precipitation was kinetically favorable by microbial activities and mineral adsorption, the sinking flux of P as vivianite in Archean seawater could have reached the modern sinking flux, implying that vivianite precipitation was a potentially major sink for P in Archean oceans. During burial diagenesis, however, vivianite in porewater would have become less stable than Ca-phosphates of lower solubility. At elevated temperatures (>100 °C) associated with burial diagenesis and low-grade metamorphism, vivianite is predicted to react irreversibly with calcite to form apatite.

Optimistic assumptions about the recycling efficiency of P on the Archean Earth lead us to estimate that by the end of the eon the total flux of P (continental weathering + recycling) could have supported NPP at levels up to 7% of the modern. The total flux of P would have been much lower on the early and middle Archean Earth, whereas fluxes of electron donors could

* Corresponding author at: Department of Marine and Coastal Sciences, Rutgers University, New Brunswick, NJ 08901, USA.
E-mail address: jihua.hao@rutgers.edu (J. Hao).

https://doi.org/10.1016/j.gca.2020.04.005

have been higher, suggesting very low productivity and P-limitation of marine ecosystems during much of the eon. Comparing our estimates of NPP as limited by P supply with the estimate by Ward et al. (2019), in which NPP was limited by electron donors and metabolic efficiency, there could have been a transition between P-limited productivity in the early to middle Archean to electron donor-limitation closer to the eon's end (assuming no oxygenic photosynthesis). Once oxygenic photosynthesis reached ecological significance, probably near the end of the Archean, our estimated flux of P would allow rapid oxidation of atmosphere.

Keywords: Vivianite; Phosphorus recycling; Burial diagenesis; Apatite nodules; Primary production; Oxygenation of atmosphere

1. INTRODUCTION

How productive were Archean oceans? All recent estimates of Archean primary production are low (Bjerrum and Canfield, 2002; Kharecha et al., 2005; Canfield et al., 2006; Laakso and Schrag, 2018; Ward et al., 2019), but there is no consensus just how low they were, nor on the principal factors that limited photosynthesis in early ecosystems. Some commentators posit that prior to the evolution of oxygenic (cyanobacterial) photosynthesis, the global availability of electron donors would have constrained rates of primary production to low levels. For example, Canfield et al. (2006) estimated the abundances of non-water electron donors in Archean oceans, concluding that the most abundant species, Fe^{2+}, would have supported primary production at levels up to 10% of the modern. In contrast, Ward et al. (2019) argued that H_2 and, to a lesser extent, Fe^{2+} together fueled early photoautotrophy at rates well below one percent of modern levels. And recently, Tosca et al. (2019) concluded that photoautotrophy of ferrous iron could have made only a negligible contribution to productivity in early oceans. In contrast, some analyses point to nutrient limitation in early oceans, specifically suggesting that relatively low phosphate availability could have limited primary production, even at low ferrous iron availability (Kipp and Stüeken, 2017); others propose that P was relatively bioavailable, especially as phosphite (Herschy et al., 2018).

Of particular interest is the role that oxygenic photoautotrophs may have played prior to the Great Oxygenation Event (GOE) ca. 2.4 billion years ago. It has been proposed that the GOE simply reflects the evolution of oxygenic photosynthesis (e.g., Kopp et al., 2005; Fischer et al., 2016), but this view is challenged by both an increasing inventory of geochemical evidence for earlier "whiffs of oxygen" (Anbar et al., 2007; Kaufman et al., 2007) and molecular clocks that call for the evolution of coupled photosystems capable of extracting electrons from water as early as 3.2 Ga (Cardona et al., 2019). Of course, if P availability strictly limited rates of primary production on the Archean Earth, oxygen production may well have been too low to titrate available reductants, even if oxygenic photosynthesis was relatively prominent.

To explore these issues further, we employ kinetic and thermodynamic modeling to estimate P availability in the global scale of seawater through a billion years of recorded Archean history.

2. METHODS

The bioavailability of P in the sunlit ocean primarily reflects two fluxes: continental weathering and P recycling within the ocean. Considering that Archean seawater was weakly acidic (Halevy and Bachan, 2017; Krissansen-Totton et al., 2018) and reducing, seafloor weathering might also have been a significant source of P on the early Earth. In Part I of this series (Hao et al., 2020), we simulated the input of P to the Archean oceans from continental weathering and erosion, concluding that P fluxes from land were extremely low as the Archean Eon began but increased to values similar to the modern by the time the eon ended. In this study, we calculate the solubility limits of primary and secondary P-minerals in Archean seawater and porewater environments, simulating seafloor weathering and the precipitation of phosphate minerals in and beneath the Archean ocean. We focus in particular on the precipitation of vivianite, as this precipitation has been argued to be a major sink for phosphate in ferruginous Proterozoic oceans (Derry, 2015). With these calculations in hand, we assess P recycling in Archean oceans and estimate the total flux of P for net primary production (NPP). Lastly, we consider the fate of P-precipitates during diagenesis and metamorphism, based on both simulations and geological observation.

Our calculations focus on the global-scale evolution of Archean environments. We understand that the Archean Earth was environmentally heterogeneous, with probable local variations in temperature, Fe(II) concentration between seawater and hydrothermal fluids, redox variation between globally anoxic and locally oxygenated habitats in the late Archean, and variations in the concentration of Fe (II) and S(II) between globally ferruginous seawater and regionally sulfidic seafloor in late Archean oceans. Such heterogeneities are important in considerations of Archean evolution and may influence Archean P cycling, as discussed below. Nonetheless, we argue that our focus on global conditions is most relevant for understanding the P cycle and how it changed through Archean time.

2.1. Archean seawater and porewater chemistry

The emergence of land masses in the middle to late Archean Eon (Hawkesworth et al., 2017), with its consequences for weathering and erosional fluxes, strongly affected marine geochemistry (Bindeman et al., 2018). The

Table 1
Fluxes of bioavailable or biological P in the modern and early Earth (in 10^{10} moles/yr).

P fluxes*	Pre-industrial Earth	Early Archean Earth	Late Archean Earth
Continental input[a]	10–15[a] (+)	~0 (+)	4–34[b] (+)
Recycling of organic P	~3710[c] (+)	<0.04 (+)	14–120 (+)[d]
Seafloor weathering[e]	10–36[f] (−)	(−)	>4 (−)
Extraterrestrial	(+)	<0.01 [g] (+)	<0.01 (+)
Total P for net primary production[h]	3720[c]	<0.05	18–154

* Plus sign (+) represents source and minus sign (−) sink.
[a] Reactive P = Dissolved inorganic P + Dissolved organic P + Particulate organic P + Iron-bound particulate P + Reactive aeolian P (Compton et al., 2010).
[b] Hao et al. (2020).
[c] Schlesinger and Bernhardt (2013).
[d] Optimisitic estimate calculated with Eqs. (8)–(10) assuming $R_{recycling} = 0.78$ (Section 3.3 in main text).
[e] Seafloor weathering (−) = hydrothermal deposition (−) + seafloor sedimentation (−) = continental input (+) + extraterrestrial input (+).
[f] Paytan and McLaughlin (2007).
[g] Tsukamoto et al. (2018).
[h] NPP(P) = continental input + recycling of organic P + extraterrestrial.

evolution of seawater pH and major salts (Ca and Mg) has recently been modeled independently by Halevy and Bachan (2017) and Krissansen-Totton et al. (2018), with similar results. In Part I of this series (Hao et al., 2020), we modified Krissansen-Totton et al.'s (2018) geologic carbon cycle (GCC) model by incorporating continental emergence (Flament et al., 2013; Korenaga et al., 2017) and the weathering kinetics of P, using this modification to simulate the continental flux of P into the oceans (Table 1). The GCC model also outputs major component compositions of the atmosphere (including $pCO_{2,g}$) and seawater (including pH, Ca^{2+}, and CO_3^{2-}), and by linking these factors to continental emergence models and solubilities of P-bearing minerals (Table S2) we can examine seafloor weathering and the precipitation of P in the Archean oceans (Section 2.2). In addition, the GCC model allows us to consider the chemistry of porewater, enabling us to explore the post-depositional fate of seafloor P-precipitates (Section 2.5).

In addition to the above-mentioned species, our simulations require that we input abundance values for other components of seawater and porewaters. A large, recently compiled dataset of fluid inclusions in Archean quartz from different localities supports the view that the concentration of NaCl in Archean seawater was similar to that of the modern (Marty et al., 2018). Accordingly, we assumed that the Cl^- concentration of Archean seawater was the same as today's. F^- concentration is set to be limited by the solubility of fluorite in Archean seawater and porewater, as it is for modern seawater.

It has been proposed that Fe^{2+} in Archean seawater was limited by the solubility of amorphous greenalite, experimentally shown to precipitate readily in equilibrium with Fe(II) and silica in anoxic water (Tosca et al., 2016; Tosca et al., 2019). Consistent with these factors, greenalite occurs abundantly in marine sediments, especially in Archean sedimentary successions (Isson and Planavsky, 2018; Johnson et al., 2018). In comparison to greenalite, siderite precipitation is kinetically sluggish under Archean conditions, occurring only when $pCO_{2,g}$ reaches extreme levels, e.g. > 1 bar (Jiang and Tosca, 2019). In the absence of a skeletal silica sink, dissolved silica concentration would presumably have been relatively high, limited by the solubility of amorphous silica (Siever, 1992; Tréguer and De La Rocha, 2012). Previous workers have also pointed to green rust as a potentially major precipitate from early seawater (Halevy et al., 2017; Tosca et al., 2019), but its precipitation requires either a flux of $O_{2,g}$ or water pH > 8.0 under anoxic conditions, unlike the anoxic and weakly acidic seawater likely during most of the Archean Eon. Moreover, the precipitation of green rust is sensitive to salinity, and the potential effects of elevated Archean $SiO_{2,aq}$ on green rust precipitation remain unknown (Tosca et al., 2019). Given these considerations, we calculated the Fe^{2+} concentration in Archean seawater based on the equilibrium constant for amorphous greenalite dissolution derived from recent experiments (Tosca et al., 2016) and the assumption that $SiO_{2,aq}$ concentration was equal to the solubility of amorphous silica. Note, however, that siderite could and did form readily by biological reduction of Fe(III) or diagenesis/metamorphism of organic-C in the sediments (Vuillemin et al., 2019), and so would potentially have been an important mineral product in porewaters beneath Archean oceans (Section 4.3).

2.2. Thermodynamic models of P-minerals solubilities

We calculated the solubility limits of common primary and secondary phosphate minerals based on equilibrium constants between each mineral and its dominant aqueous species at a given pH in water, e.g. HPO_4^{2-} (pH > 7.2) and $H_2PO_4^-$ (pH < 7.2) as the dominant phosphate species in this study (Tables S1 and S2). Calculations were conducted assuming a warm climate (seawater temperature 25 °C), supported by recent climate reconstructions (Krissansen-Totton et al., 2018). Small fluctuation of temperature would be expected to result in only limited changes for reaction constants (e.g. Al-Borno and Tomson, 1994). However, large elevation of temperature would significantly affect reaction constants; therefore, for the calculations in diagenetic and metamorphic environments, we varied temperature to investigate the effect of this variable (see below). Equilibrium constants of the dissolution

reactions were calculated by SUPCRT92b (Johnson et al., 1992) (Table S2).

In the modern ocean, the sinking of P is, in general, composed of (co-)precipitation of authigenic minerals (Table S1), burial as organic-P, or adsorption onto metal-hydroxides and carbonate (Baturin, 2003; Ruttenberg, 2014). In iron-rich, low-salinity estuaries along the Baltic Sea, vivianite ($Fe_3(PO_4)_2$*$8H_2O$) precipitation accounts for as much as 40% of P removal from ambient waters (Lenstra et al., 2018), and Derry (2015) has proposed that this mineral formed an important sink for P in the ferruginous, low-sulfate seawater of mid-Proterozoic oceans. Derry's hypothesis may apply, as well, to the Archean, but this possibility needs to be tested for the distinct and evolving conditions of Archean seawater (pH, Fe, S, and silica). The solubility constant of vivianite is adopted from a previous experimental study (Al-Borno and Tomson, 1994).

$$Fe_3(PO_4)_2{\cdot}8H_2O_{,s} \rightarrow 3Fe^{2+} + 2PO_4{}^{3-} + 8H_2O \quad (1)$$

At $pH < 7$, $PO_4^{3-} + 2H^+ \rightarrow H_2PO_4^-$. As mentioned above, seawater Fe(II) is presumably controlled by the solubility of amorphous greenalite:

$$Fe_3Si_2O_5(OH)_{4,am} + 6H^+ \rightarrow 3Fe^{2+} + 2SiO_{2,aq} + 5H_2O \quad (2)$$

where, $SiO_{2,aq}$ is set by the solubility of amorphous silica:

$$SiO_{2,am} \rightarrow SiO_{2,aq} \quad (3)$$

We can obtain the equilibrium constant of the following reaction by combining the reaction constants of reactions (1)–(3):

$$Fe_3(PO_4)_2{\cdot}8H_2O_{,s} + 2SiO_{2,am} \rightarrow Fe_3Si_2O_5(OH)_{4,am} + 2H_2PO_4{}^- + 2H^+ + 3H_2O \quad (4)$$

In similar fashion, we compiled the reported equilibrium constants of the dissolution reactions of other common secondary P-minerals and calculated their solubility limits in the Archean seawater and porewater (Table S2).

2.3. Crystallization and precipitation kinetics of vivianite

We employed the crystal growth kinetics of vivianite reported previously (Madsen and Hansen, 2014; Madsen, 2019). Vivianite crystals have shown to follow spiral growth mechanism at low supersaturation states (Madsen and Hansen, 2014) with the rate expression:

$$Rs = b\left(c_{Fe} - c_{Fe,eq}\right) ln\Omega \quad (5)$$

b (nm/s/M) is rate constant, Ω is the saturation state of vivianite defined by the ratio of quotient (Q) and equilibrium constant (K) of the precipitation reaction. Considering that the Archean seawater had high concentrations of Fe^{2+} and vivianite could reach moderate to high supersaturation states (as discussed below), we assume that $c_{Fe} - c_{Fe,eq} \cong c_{Fe}$. The value of b was found to increase with increasing concentrations of Ca^{2+}; due to the limited Ca^{2+} range considered in the literature, we used 3.19 (at 6.11 mM Ca^{2+} in Madsen & Hansen, 2014) as a conservative value for Archean seawater.

Following the methods proposed by Derry (2015), we simulated the precipitation rate and deposition flux of vivianite as a function of this mineral's saturation state. Simply put, the rate law for vivianite precipitation is

$$R_p = k_{eff}\left[\left(\frac{Q}{K}\right) - 1\right]^n \quad (4)$$

R_p: precipitation rate of vivianite, mole/(m^3*s); k_{eff}: $2.6 \pm 0.3 \times 10^{-15}$ mol/(m^3*s); n: 1.3 ± 0.3. The precipitation flux of vivianite is calculated by integrating the rate over the likely depth of Archean Fe(II)-rich seawater, similar to Derry (2015).

2.4. Recycling of phosphorus in Archean seas

Considering that seafloor weathering (Sections 3.1 and 4.1) and extraterrestrial impacts (Table 1) provide only small amounts of phosphorus, we assume that the total P for Archean NPP is predominantly composed of P from continental weathering and recycling within the ocean, i.e.,

$$\text{NPP(P)} = \text{Recycling} - \text{P} + \text{Weathering} - \text{P} \quad (5)$$

Assuming $R_{recycling}$ = recycling efficiency of biological P,

$$\text{Recycling - P} = R_{recycling} * \text{NPP(P)} \quad (6)$$

Therefore,

$$\text{NPP(P)} = R_{recycling} * \text{NPP(P)} + \text{Weathering - P} \quad (7)$$

And,

$$\text{NPP(P)} = \text{Weathering} - \text{P}/\left(1 - R_{recycling}\right) \quad (8)$$

According to Table 1, $R_{recycling} = 0.998$ in the modern ocean, but due to a limited supply of oxidants and possible precipitation of P as vivianite in the Archean ocean, the recycling of P would have been less efficient. As discussed in detail in Section 4.4, we choose $0.01 < R_{recycling} < 0.78$ in the Archean ocean and, based on that value, we calculate the maximum amount of recycled P available for Archean primary producers, as reported in Table 1.

2.5. Diagenetic and metamorphic transformation of vivianite: modeling

In this study, we simulated the stability and solubility of various phosphate minerals and other diagenetic minerals in porewater environments (Fig. S1-2; 25 °C), thereby mimicking the early diagenesis of P in the Archean marine sediment.

In addition, we simulated the reaction of vivianite + calcite (+fluorite as a source of F^-) to form apatite + siderite (+release of water) at elevated temperatures, mimicking the fate of vivianite during burial diagenesis and metamorphism. The equilibrium constants of the reaction were calculated by SUPCRT92b, with thermodynamic properties of vivianite from Al-Borno and Tomson (1994).

3. RESULTS

3.1. Limitations on seafloor weathering of apatite

In continental rocks, apatite is the primary P-hosting mineral for chemical weathering, and detrital P, mainly as apatite, is the predominant component of continental P input to the ocean system (Compton et al., 2010; Ruttenberg, 2014). In oceanic crust, apatite is unlikely to be a major host mineral for P due to high saturation concentrations; rather P is expected to exist either as trace impurities in silicate minerals — including olivine, clinopyroxene, and plagioclase — or in basaltic glass (Brunet and Chazot, 2001). However, trace amounts of apatite are common in basalts and gabbros (e.g., Anderson and Greenland, 1969; Coogan et al., 2001; Meurer and Natland, 2001), and apatite may precipitate locally due to the P gradient near a growing crystal (Green and Watson, 1982).

If the concentration of dissolved P in the weathering fluid reaches the solubility limit of apatite, apatite as the reactant will have no reaction affinity to dissolve further (Brantley and Olsen, 2014). Salinity and pH are the two most important environmental determinants of apatite solubility. Seawater pH is primarily buffered by the riverine transport of alkalinity, seafloor weathering of silicates, and hydrothermal fluids. Although the Archean atmosphere had high $pCO_{2,g}$, simulated pH of Archean seawater ranges from 6.5 to 7.0 (Halevy and Bachan, 2017; Krissansen-Totton et al., 2018), unlike the more acidic rainwater that drove continental weathering (Hao et al., 2017). Ca^{2+} level is another important factor in determining the solubility of P. It has been proposed that Archean seawater was more enriched in Ca^{2+} than the modern oceans because of enhanced hydrothermal alteration of the seafloor (Jones et al., 2015; Halevy and Bachan, 2017; Krissansen-Totton et al., 2018).

Based on these considerations, and applying our additional assumptions for Archean seawater composition (Methods), we calculated the solubility limits for three common types of apatite: Cl-apatite, F-apatite, and OH-apatite. Fig. 1 shows that all three minerals had limited solubility (<0.1 μM; predominantly as $H_2PO_4^-$ at pH < 7) in Archean seawater; results are consistent whether one assumes rapid or slow continental emergence on the late Archean Earth. The low solubility of apatite minerals in Archean seawater contrasts markedly with their high solubilities in contemporaneous continental weathering fluids (Hao et al., 2017), a difference primarily ascribed to the higher pH and higher concentrations of Ca^{2+} and halogens in Archean seawater, relative to rain or river water (Hao et al., 2020). In addition, the log dissolution rate of apatite minerals decreases linearly with increasing pH in acidic water (Guidry and Mackenzie, 2003; Brantley and Olsen, 2014). Thus, in Archean oceans, the weathering of apatite was both thermodynamically and kinetically less favorable than continental weathering. Indeed, the direct implication of Fig. 1 is that seafloor weathering of apatite minerals could have contributed little if any P to early marine life. Consistent with these simulation results, we observed detrital apatite as the major P-phase in Archean black shales, with tiny overgrowths of secondary apatite (Bothaville Formation, South Africa; ca. 2700 Ma) (Fig. 7a and b). Bothaville sediments reflect rapid uplift and erosion of a crustal bloc to the west (Schneiderhan et al., 2011), resulting in large input of P with a major proportion being detrital apatite minerals (Hao et al., 2020). In addition, as discussed in Section 4.1, we think that seafloor weathering of basalt would contribute little P to early oceans.

3.2. Solubility and precipitation of secondary phosphates in the Archean seawater

On the modern Earth, seafloor weathering serves as a net sink for P that balances continental input (Compton et al., 2010), with P removal occurring mainly as organic-P, various authigenic/biogenic phosphate minerals (CFA, HAP, and other phosphates), and surface adsorption onto or co-precipitation with Fe(III)-(hydr)oxide and carbonate

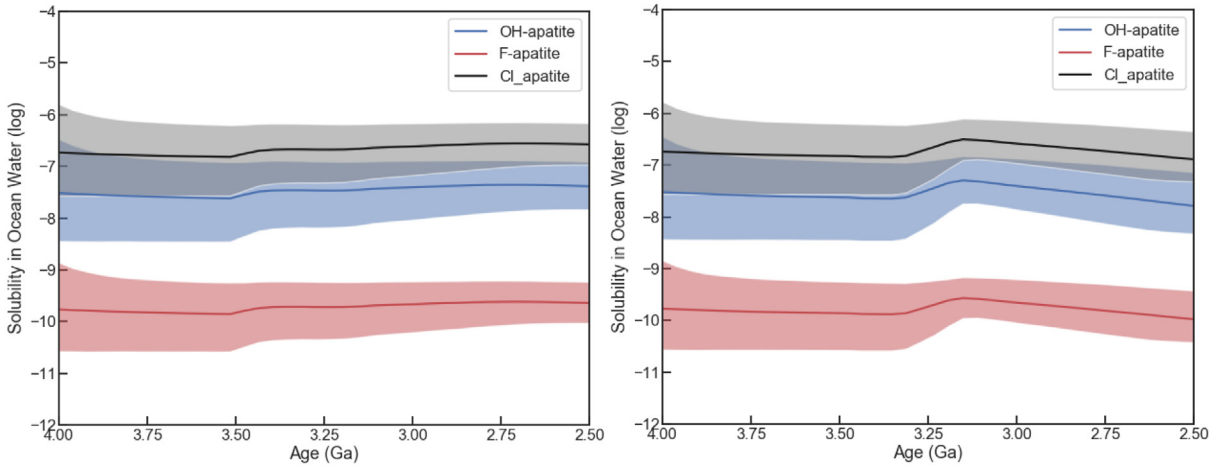

Fig. 1. Limited solubilities of apatite minerals in the Archean seawater conditioned by the model of a. slow continental emergence late in the Archean Eon (Flament et al., 2013); b. rapid continental emergence late in the Archean Eon (Korenaga et al., 2017). Solid lines show median outputs, and shaded regions show 95% confidence intervals.

(Ruttenberg 2014). In anoxic Archean seawater, Fe(II) oxidation could and did occur via photo- and/or bio-oxidation of Fe(II), or the cooling of hydrothermal fluids, as documented by ferric iron in Archean banded iron formations. Several investigators analyzed the P content in BIFs in order to reconstruct paleo-concentrations of P, assuming that adsorption onto Fe-(hydr)oxide was the major sink for P (Konhauser et al., 2007; Planavsky et al., 2010; Jones et al., 2015).

In addition to surface adsorption, however, our simulations suggest that vivianite would have a much lower solubility in Archean seawater than other secondary P-minerals (e.g. octacalcium phosphate, or OCP) (Table S1 and Fig. 2). Assuming a moderate supersaturation state of vivianite, $\Omega = 100$ or 1000, our calculations indicate that phosphate solubility in Archean oceans would have been similar to that estimated by Jones et al. (2015), 0.1–0.3 μM dissolved phosphate depending on Ω and age (Fig. 2). This estimate depends heavily on the feasibility of vivianite precipitation, experimentally shown to be sluggish at low supersaturation but potentially facilitated by microbial reduction and mineral adsorption in natural systems (Section 4.2). Regardless, in the low-P Archean seawater, octacalcium phosphate (OCP) as the precursor phase of marine apatite (Van Cappellen and Berner, 1991) has no thermodynamic affinity to precipitate. Undersaturation of OCP in the Archean seawater further indicates that, precipitation of apatite minerals, although thermodynamically favorable given their extremely low solubilities (Fig. 1), was not kinetically feasible (Gunnars et al., 2004).

Using the reported crystallization kinetics of vivianite (Madsen and Hansen, 2014; Madsen, 2019) and assuming the presence of mineral seed, we estimated 46–695 μm crystal growth for 1 year at supersaturation states of 100–1000 in the Archean seawater (Fig. 3a; assuming 0.1–1 mM Fe^{2+}), this falling into the size range of vivianite nodules found in natural sediments at low supersaturation states (Rothe et al., 2016). Following the method proposed by Derry (2015), we calculated the precipitation rate of vivianite from water column to sediment, showing that the depositional flux of P as vivianite in the Archean oceans could easily have reached levels comparable to the modern sinking flux for P at $\Omega > 10$ (i.e., solubility of $P = 0.03$ μM) (Fig. 3b). Derry's model assumes ready vivianite precipitation even at low supersaturation states, but the actual precipitation flux should depend heavily on precipitation kinetics of vivianite, which is known to be affected by a number of factors (Section 4.2).

3.3. Post-depositional transformation of vivianite

As discussed above, vivianite precipitation could be an important P sink in Archean oceans. The fate of vivianite during diagenesis and metamorphism, however, requires consideration.

Assuming that siderite and greenalite precipitation could reach in equilibrium, our simulations show that in the porewater environment siderite solubility is 2 to 4 orders of magnitude lower than greenalite (Figs. 4a and S3a). Therefore, if siderite precipitation becomes kinetically feasible during burial diagenesis (Section 4.3), it should limit the solubility of Fe(II) to low values, as argued for Archean porewaters (Tosca et al., 2019). Under these conditions, vivianite becomes much more soluble than other secondary phosphate minerals, e.g. octacalcium phosphate (OCP) and carbonate fluorapatite (francolite) (Figs. 4b and S3b). OCP is thought to be the precursor phase of marine apatite minerals (Eanes and Meyer, 1977; Van Cappellen and Berner, 1991). In the modern marine sediments, precipitation of P as apatite minerals is thought to one major P sink in the long run (Ruttenberg, 2014; Van Cappellen and Berner, 1991). Our simulations show that in the Archean porewaters, the solubilities of apatite minerals are expected to be extremely low (at least 1–3 orders of magnitude lower than OCP and 5–9 orders of magnitude lower than vivianite; Fig. 4c), implying strong thermodynamic affinity for the transformation from vivianite to OCP and apatite minerals (Sec 4.3).

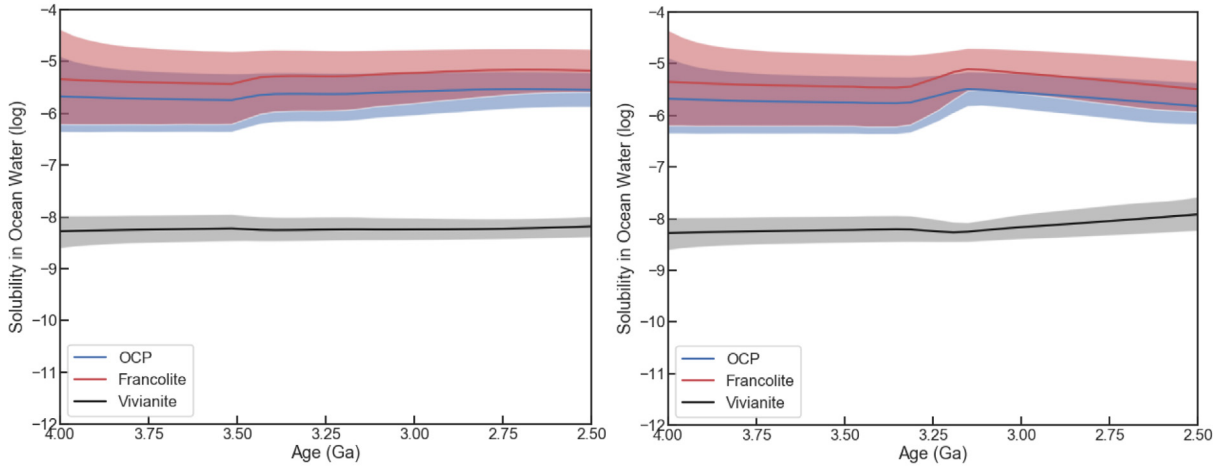

Fig. 2. Solubilities of various secondary-P minerals in the Archean seawater conditioned by the model of a. slow continental emergence late in the Archean Eon (Flament et al., 2013); b. rapid continental emergence late in the Archean Eon (Korenaga et al., 2017). Solid lines show median outputs, and shaded regions show 95% confidence intervals.

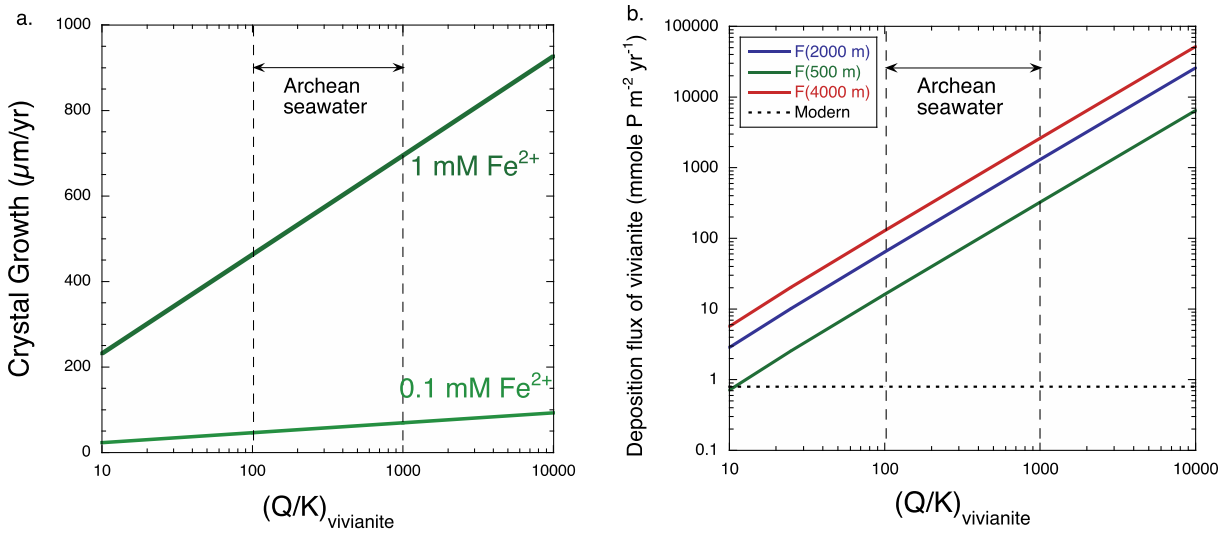

Fig. 3. Precipitation of vivianite in Archean seawater: a. spiral growth (μm/yr) and b. deposition flux of P as vivianite, as a log function of the probable range of supersaturation states (Q/K) of vivianite and the thickness of the Archean ferruginous water column (colorful lines in b). Dashed line in b shows the depositional flux of P in the modern ocean. Methods adopted from Derry (2015).

In addition, we calculated the reaction constant for the transformation of vivianite + calcite (+fluorite; with a fluorine level similar to the seawater) to F-apatite + siderite (with release of water) at elevated temperatures, mimicking the burial diagenesis and low-grade metamorphism of vivianite. The result suggests that log (reaction constant) is $\gg 1$, and its value increases with temperature (Fig. 5), suggesting that the transformation becomes thermodynamically more and more favorable. Therefore, it can be reasonably expected that at the elevated temperatures of burial diagenesis and metamorphism (>100 °C, where the precipitation kinetics of apatite and siderite are feasible), vivianite would inevitably transform to apatite.

3.4. Total phosphorus for Archean primary production

Fig. 6 shows the proportional contribution of continental weathering to the total P requirement for NPP as a function of recycling efficiency. In line with the hypothesis by Laakso and Schrag (2018), the figure indicates that on the Archean Earth, continental weathering would provide the major source of P for life in photic zone, unlike today. Based on our estimate of continental P flux (Table 1) and a recycling efficiency of 0.78 (Section 4.4), we calculate the recycling flux of organic P by the end of the Archean Eon to have been 14–120 $\times$ 10^{10} moles P/yr (Table 1). Note that the flux of recycling P, which represents an optimistic estimate in this study, depends heavily on the recycling efficiency (and thus burial efficiency) of organic matter in the Archean Eon, which is poorly constrained (Kipp, 2019) and might have evolved through time (Section 4.4). Assuming deep water P concentrations equivalent to 10% of the modern value and a typical vertical mixing rate (3 m/yr), Ward et al. (2019) recently estimated Archean P recycling to have been 40 $\times$ 10^{10} moles P/yr, within the range of our values. Regardless of uncertainties, these estimates agree that the recycling flux of P in late Archean oceans was 1–2 orders of magnitude lower than today's (about 3710 $\times$ 10^{10} moles P/yr; Schlesinger and Bernhardt, 2013). Together with our estimated continental input of P, up to 18–154 $\times$ 10^{10} moles P/yr would have been available for marine primary productivity by the end of Archean Eon, 0.5–4% of modern values (Table 1). Because of limited continental emergence and elevation, the continental flux of P and thus the recycling flux of P would have been much smaller on the earlier Archean Earth, perhaps $< 0.05 \times 10^{10}$ moles P/yr, i.e. 0.001% of the modern value (Table 1).

4. DISCUSSION

4.1. Seafloor weathering of phosphorus

In the modern ocean, seafloor weathering is widely agreed to be a net sink for P, primarily due to surface adsorption onto Fe(III)-hydroxide or carbonate (Wheat et al., 1996) or (co)precipitation of P-minerals (hydroxylapatite, CAP, REE/Al-phosphates) (Ruttenberg, 2014). Given the reducing and weakly acidic nature of Archean seawater, however, dissolution of basaltic glass has been proposed as a source of P for autotrophs (Kakegawa, 2003). To date, there is limited evidence to support this hypothesis. Syverson et al. (2020) recently observed slight P release during alteration of basalt at 25 °C under anoxic conditions, whereas alteration experiments under oxic condition did not show any P release. These observations seemingly support seafloor weathering as a potential source of P in the anoxic Archean ocean(s). However, Syverson et al. used a simulated seawater solution without any inorganic C, which diverges markedly from realistic estimates of Archean seawater chemistry (high $CO_{2,aq}$ and (bi)carbonate species; Halevy and Bachan, 2017; Krissansen-Totton et al., 2018). Under these more realistic conditions, seafloor weathering would precipitate abundant carbonate minerals, a major sink in the Archean carbon cycle (Krissansen-

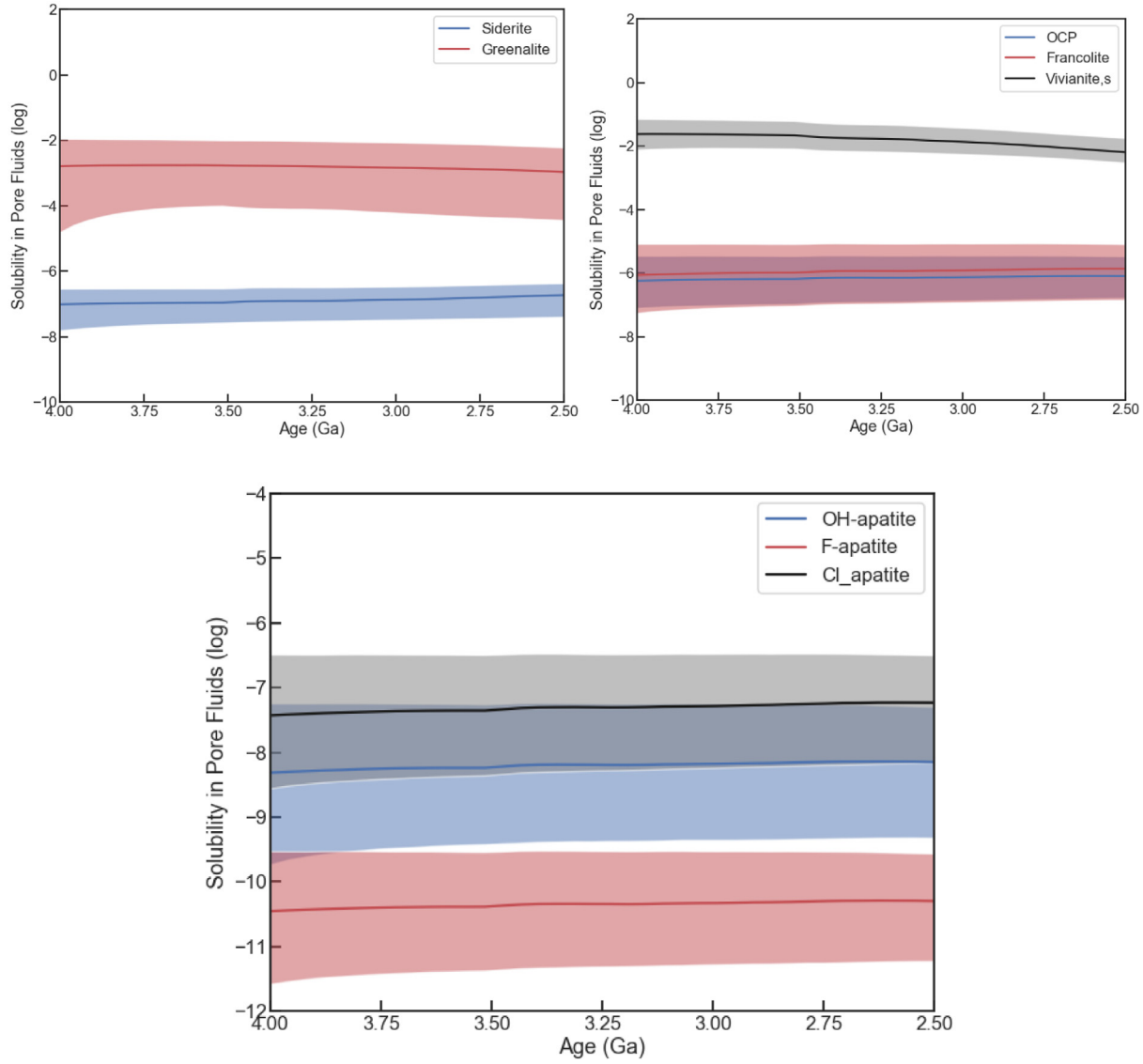

Fig. 4. Solubility of siderite and greenalite (a), secondary phosphate minerals (b), and apatite minerals (c) in porewater conditioned by the model of slow continental emergence in the late Archean (Flament et al., 2013). The case of rapid continental emergence in the late Archean (Korenaga et al., 2017) is shown as supplementary Fig. S3 with similar trajectories. Solid lines show median outputs, and shaded regions show 95% confidence intervals.

Totton et al., 2018) as well as a known mineral product in modern seafloor weathering. Carbonate minerals have a strong affinity to phosphate and could limit soluble P by either surface adsorption (de Kanel and Morse, 1978; Wheat et al., 1996; Millero et al., 2001) or co-precipitation as carbonate apatite (Freeman and Rowell, 1981; Rubinstein et al., 2013; Xu et al., 2014); both represent a major sink for P in modern carbonate-rich and/or anoxic sediments (e.g. Baturin, 2003; Fourqurean et al., 1992; Kraal et al., 2017). In addition, elevated temperature or presence of divalent cations (e.g. Ca^{2+}, Mg^{2+}) would increase uptake of phosphate by carbonate (Millero et al., 2001). In fact, carbonate minerals can capture 2.3–4.5 * 10^{12} mole P/yr in the modern ocean, 2–4 times the sink provided by hydrothermal iron hydroxides (Baturin, 2003); carbonates could be expected to form a larger sink in the Archean due to higher $pCO_{2,g}$ and highly weatherable rocks.

In another study, Murakami et al. (2019) investigated the hydrothermal alteration of basalt under CO_2-rich condition (+30 mmole/kg Ca^{2+}), mimicking Archean atmospheric and seawater composition. Their experiments revealed under high CO_2 conditions, carbonate was a major alteration product, with higher P-uptake than occurred in a CO_2-free run, supporting the hypothesis that carbonate minerals would take up phosphate released from seafloor weathering or via diffusion from seawater. A limited contribution of P from glass weathering is further supported by

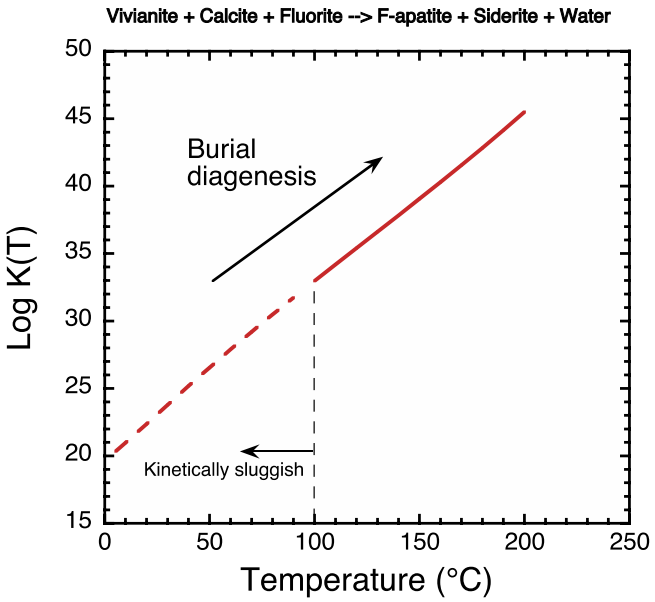

Fig. 5. Transformation of vivianite into apatite during diagenesis and metamorphism: equilibrium reaction constants of vivianite together with calcite and fluoride to form apatite and siderite at elevated temperatures. Dashed red line indicates sluggish reaction kinetics due to kinetic inhabitation of apatite and siderite precipitation at low temperatures. (For interpretation of the references to colour in this figure legend, the reader is referred to the web version of this article.)

the observations of modern and Archean glasses altered under anoxic conditions; these showed enrichment or no loss of P (Alt and Honnorez, 1984; Rubinstein et al., 2013; Staudigel et al., 2008). In addition to uptake by carbonates, there are other substantial sinks of P during seafloor weathering, including the precipitation of Al/REE phosphates (Byrne and Kim, 1993; Rasmussen, 2000) and vivianite (this study; Derry, 2015). Based on the above considerations, we argue that seafloor weathering should be a negligible source and possibly a large sink in the Archean P cycle.

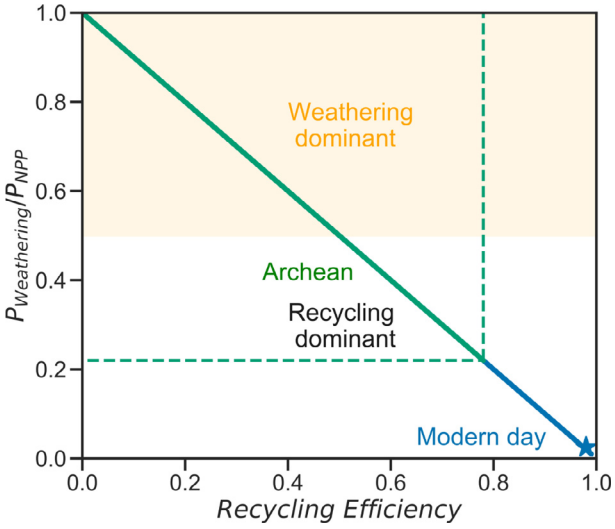

Fig. 6. Proportional contribution of continental weathering flux to the total P requirement of primary production plotted against recycling efficiency ($R_{recycling}$ = Recycling-P/Net primary production P) of organic-P in seawater. Blue line indicates the range of modern water bodies from anoxic lake ($R_{recycling}$ = in 0.78 in ferruginous Lake Matano; Crowe et al. 2011; Katsev and Crowe, 2015) to oxic seawater (star; $R_{recycling} = 0.998$). The green line shows our proposed Archean case ($0.01 < R_{recycling} < 0.78$; see Section 4.4 for discussion), in which P recycling was limited within ferruginous water. (For interpretation of the references to colour in this figure legend, the reader is referred to the web version of this article.)

4.2. Vivianite precipitation kinetics

Direct precipitation of vivianite from Fe(II)-PO_4 solution has been experimentally shown to be kinetically inhibited at low saturation states under ambient conditions (Walpersdorf et al., 2013). In addition, at low supersaturation states, vivianite precipitation has been shown to follow spiral growth mechanism, at rates slower than surface-nucleation growth at high supersaturation states (Madsen and Hansen, 2014; Madsen, 2019). Altogether, slow kinetics of precipitation and crystallization might indicate a relatively minor role for vivianite as a P sink in Archean oceans. Indeed, Johnson et al. (2020) suggested that vivianite was not a major P sink in the ferruginous sediments of the Mesoproterozoic Sherwin Ironstone despite the high supersaturation states predicted by thermodynamic models. However, in modern Fe(II)-rich anoxic waters (Cosmidis et al., 2014) and sediments (Borch and Fendorf, 2007; Jilbert and Slomp, 2013; Sánchez-Román et al., 2015), vivianite precipitation can be facilitated by microbial reduction of Fe(III) in presence of phosphate. In addition, phosphate adsorbed into ferrous minerals, e.g. green rust, has been shown to quickly transform into vivianite (Hansen and Poulsen, 1999; Xiong, 2019). The presence of mineral seeds (e.g. quartz) could also facilitate the crystallization

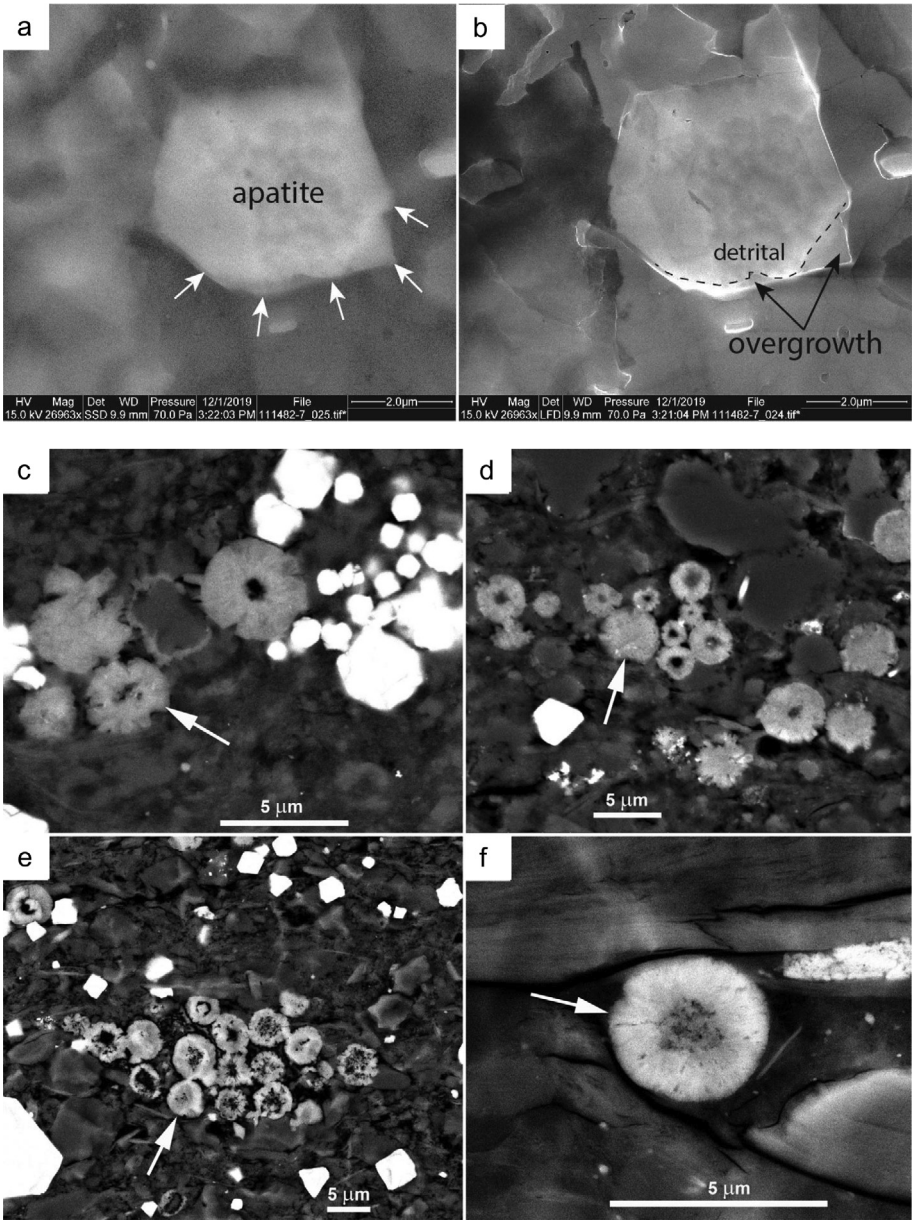

Fig. 7. Contrasting appearance of apatite grains from Archean and Mesoproterozoic Archean and Mesoproterozoic carbonaceous shales as imaged by scanning electron microscope (SEM). (a) Bothaville Formation (ca. 2700 Ma), South Africa, apatite grain in center (white arrows), backscatter electron image. (b) Charge contrast in secondary electron mode allows differentiation between detrital grain and diagenetic overgrowth (dashed line) that extends into surrounding pore space. (c) Newland Formation (Belt Supergroup, Montana, USA). Note deformed thin-walled "sphere" in center of image, as well as apatite crystals projecting beyond sphere outlines. (d) Bijaigarh Shale, Vindhyan Supergroup, India, with some deformed shells and apatite crystals projecting beyond sphere outlines. (e) Velkerri Formation, Roper Group, Australia; note deformed thin-walled "spheres". (f) Solid sphere with less mineralized center portion, Kaltinsky Formation Siberia. With exception of image (b), all images were acquired with a scanning electron microscope (SEM) in backscatter mode.

of vivianite and lower the supersaturation demand (Liu et al., 2018). These mechanisms may explain the precipitation of vivianite at low to moderate supersaturation states in modern anoxic waters ($\Omega = 40$ for lake Pavin; Cosmidis et al., 2014) and sediments ($\Omega < 1$ for Baltic Sea porewater; Jilbert and Slomp, 2013; $\Omega < 1000$ for Lake Groß-Glienicke and Lake Arendsee porewaters, although Lake Spitzingsee porewater vivianite is absent at $\Omega > 10000$; Rothe et al., 2016), which might also have been true for Archean oceans.

Given these uncertainties, we cannot provide a quantitative estimate for the sedimentation flux of phosphate as vivianite in Archean oceans and thus evaluate the importance of vivianite precipitation as a P sink. Global vivianite fluxes would be greatly affected by poorly constrained concentrations and fluxes of phosphate and ferrous iron in

Archean seawater. Moreover, the precipitation kinetics of vivianite are strongly influenced by temperature (Madsen and Hansen, 2014), microbial activity (Borch and Fendorf, 2007), and mineral surface (Hansen and Poulsen, 1999; Liu et al., 2018; Xiong, 2019). Additionally, adsorption onto Fe-(hydr)oxide (Bjerrum and Canfield, 2002; Jones et al., 2015) or green rust (Zegeye et al., 2012) and/or co-precipitation as Fe(III)-phosphate would have competed for P with vivianite precipitation in surface seawater, and these processes cannot be quantified on the basis of available information. Nevertheless, we support the qualitative argument that the global flux of P precipitated by vivianite was important in the Archean P cycle, limited largely by the input of P from continental weathering and riverine transport (Table 1).

4.3. Burial of P in the Archean marine sediments

Within sediments, precipitation of siderite could become kinetically feasible during diagenesis through bioreduction of Fe(III) in the presence of organic matter (Vuillemin et al., 2019) or via burial heating. Our simulations suggest that siderite precipitation would minimize the solubility of Fe(II) (Fig. 4a); as a result, sedimentary vivianite would have higher solubility than calcium phosphates (Fig. 4b and c). Under these circumstances, vivianite becomes unstable with respect to calcium phosphates, and the dissolution of vivianite could result in higher P than OCP and francolite solubility in porewater (Thinnappan et al., 2008), inducing OCP or francolite precipitation. OCP has been suggested as essential precursor phase for apatite precipitation (Gunnars et al., 2004; Van Cappellen and Berner, 1991) and the presence of OCP could facilitate the precipitation of apatite, which would continue until P levels declined to values lower than OCP solubility (Nancollas, 1984; Van Cappellen and Berner, 1991). Given the much lower solubility of apatite minerals than vivianite and OCP (Fig. 4c), precipitation of apatite should be a significant P-sink, maintaining low levels of P in Archean porewater (<1 μM as the solubility of OCP in Fig. 4b).

Other forms of deposited P, including Fe(III)/Al-hydroxide or carbonate bound- and organic-P, might also transform into calcium phosphates, along with the reduction of Fe(III) and breakdown of organic matter in porewater environments. Indeed, transformation of Al/Fe (III)-bound P to OCP has been observed in modern nearshore sediments and shown to be facilitated by increasing pH and/or decreasing Eh (Oxmann and Schwendenmann, 2015). In modern anoxic sediment, it has been observed that organic-P could transform progressively into calcium phosphate with the aid of $CaCO_3$ during burial diagenesis (Kraal et al., 2017). Archean porewaters were probably enriched in Ca (Fig. S1-2) and enhanced seafloor weathering at high $pCO_{2,g}$ would induce widespread precipitation of $CaCO_3$ in sediments (Sleep and Zahnle, 2001). Thus, as argued for vivianite, organic-P would also transform into calcium phosphates during burial diagenesis, depending on the relative concentrations of Ca^{2+} and Fe^{2+} and ambient pH in sediments. Recently, Johnson et al. (2020) reported carbonate fluorapatite as the major phosphate in a Mesoproterozoic ferruginous sediment, probably transformed from Fe(III)-bound or organic P during burial diagenesis, supporting the hypothesis that precipitation of calcium phosphates as the dominant long-term P-sink.

We also note that the present day mineralogy of iron formations is thought to bear the strong imprint of diagenesis, including supergene enrichment (Rasmussen et al., 2016). Therefore, the current Fe and P mineralogy of Archean BIFs may not provide a strong test of our or any other low-temperature environmental hypotheses. Ca-rich carbonate would be a major product of seafloor weathering under a high $pCO_{2,g}$ Archean atmosphere (Sleep and Zahnle, 2001), its solubility increasing with rising burial pressure. $CaCO_3$ dissolution has been shown to aid long-term sequestration of P in the sediments of modern anoxic basins by facilitating the precipitation of Ca-P minerals (Krajewski et al., 1994; Kraal et al., 2017). Therefore, in the long term, progressive burial might have converted vivianite to less soluble apatite.

Consistent with these considerations, tiny spheroids of apatite (Fig. 7) have been observed in Archean and Proterozoic carbonaceous shales (several% TOC) from multiple and widely separated localities. These spheroids typically measure 2–5 micrometers in diameter and may form solid spheres as well as thick- or thin-walled shells (Fig. 7). The illustrated Archean example (Bothaville Formation, South Africa; ca. 2700 Ma) shows predominantly detrital grains with small later diagenetic overgrowths (Fig. 7a-b). In essence, this coexistence suggests that apatite was originally deposited as a detrital component from continental erosion; in places where P concentrations reached saturation for apatite overgrowth, diagenetic overgrowths started to fill in adjacent pore space. In contrast to the Archean samples, common to all of the Proterozoic precipitates are micron-sized spheres or shells that consist of radiating apatite crystals that in places may extend beyond the apparent original sphere or shell margin outline (Fig. 7c-f). Thin-walled shells commonly show variable degrees of deformation, suggesting that apatite nucleated on partially degraded cell walls or extracellular envelopes. In places, multiple spheres are joined together to form a single mineralized entity (Schieber et al., 2007). The clustering of spheroids (Fig. 7c, d, e), the apparent progression from mineralized membranes, to thick-walled shells and solid spheres (Fig. 7f), and the commonly observed association with organic matter are suggestive of an organic origin, possibly as mineralized microbes that were associated with decaying organic matter (Schieber et al., 2007).

The microspheres are consistent with P liberation during organic remineralization, followed by vivianite/OCP precipitation and, later, eventually transformation to apatite during diagenesis, although we cannot reject the alternate possibility that phosphorus precipitated originally as apatite. In either case, however, P liberated by organic remineralization did not return to the water column, but rather was immobilized by mineral precipitation.

In recent experiments, Herschy et al. (2018) documented the partial reduction of orthophosphate (PO_4^{3-}) into phosphite (PO_3^{3-}) by Fe(II) at 180 °C, mimicking burial diagenesis. This mechanism is possible, but it has little influence

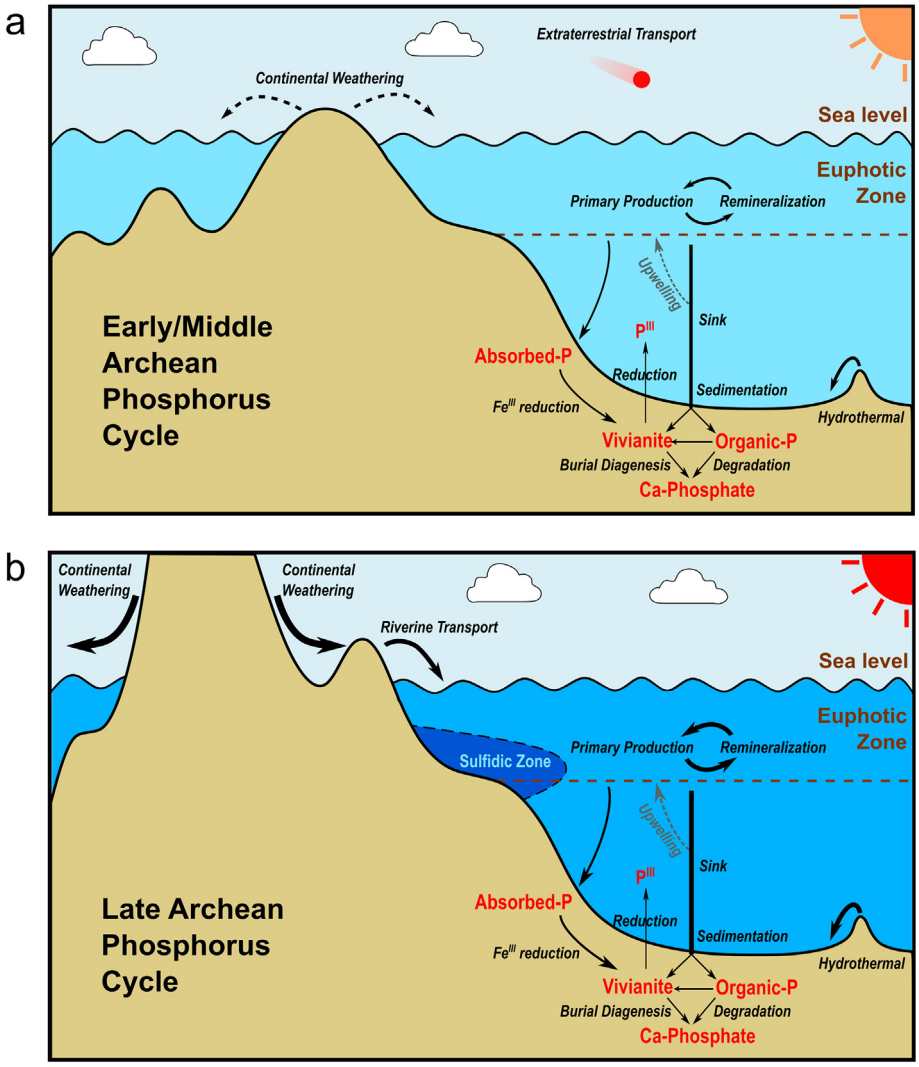

Fig. 8. Reconstructed phosphorus cycle in the early/middle Archean (a) and late Archean (b) worlds. The intensity of seawater color indicates relative levels of P, i.e. thin blue, medium blue, and dark blue represent low, medium, and high P concentration, respectively. Arrow weights indicate the relative flux of constituent processes within the P cycle (smaller flux by thin lines and greater flux by thick lines). Dashed lines or regions indicate processes presumed to be weak or only expressed locally. (For interpretation of the references to colour in this figure legend, the reader is referred to the web version of this article.)

on our conclusions, as even under favorable conditions only about 5% of precipitated phosphate would be reduced to phosphite (Herschy et al., 2018). We note as well that the research in question did not include Ca (either aqueous species or carbonate) in the experimental system. Ca would significantly favor the stability of apatite $Ca_5(PO_3)_3(OH,F,Cl)$ against reduction of orthophosphate at the elevated temperatures and pressures associated with diagenesis and low-grade metamorphism (Fig. 5). This inference is consistent with evidence that apatite is the dominant P-mineral in ancient sedimentary rocks (Lepland et al., 2002; Friend et al., 2008).

4.4. Recycling of P in the Archean ocean

In the modern ocean, continental input of bioavailable P accounts for less than 1% of the P requirement for net primary production (NPP) (Table 1; Schlesinger and Bernhardt, 2013); the recycling of biological phosphate within the ocean overwhelmingly dominates P supply to the photic zone. On the Archean Earth, however, when the atmosphere and oceans were largely reducing, a lack of oxidants would have suppressed the recycling efficiency of biological P (Kipp and Stüeken, 2017). And, as already introduced, our simulation shows that precipitation of secondary phosphates as vivianite or Ca-phosphates might also maintain low concentrations of dissolved P in Archean seawater and porewater, impeding the recycling of phosphate freed via organic matter remineralization. Therefore, the recycling of biological P was very likely much weaker in Archean oceans and, accordingly, NPP must have been much lower.

The recycling efficiency of organic matter is inversely proportional to the burial efficiency of NPP, which depends

on the availability of oxygen (Hedges et al., 1999) and other oxidants, as well as bioturbation (Zonneveld et al., 2010). Indeed, burial efficiency has an inverse relationship with exposure of oxygen (as well as other oxidants), and extrapolation of the correlation to zero oxygen exposure results in 40–50% burial efficiency (Hartnett et al., 1998). Moreover, it has been estimated that burial efficiency can be as high as 22–32% in modern ferruginous lakes (Crowe et al., 2011; Katsev and Crowe, 2015; Kuntz et al., 2015), although transferring this estimate to the entire ocean needs further investigation. In contrast, the burial efficiency of oceanic NPP is about 0.1% in modern oceans (Hedges and Keil, 1995).

Modern lakes certainly have greater inventories of oxidants (O_2, SO_4^{2-}, NO_3^-) than Archean seawater. Input of sulfate would also undermine the burial P as vivianite by lowering the solubility of Fe(II) in anoxic waters and sediments (Rothe et al., 2015); however, the Archean seawater was depleted in sulfate (Lyons and Gill, 2010). Such considerations suggest that the recycling efficiency of biological P would have been even lower in Archean oceans than in modern ferruginous lakes, i.e. $R_{recycling} < 0.68$–0.78 in the Archean (Fig. 6). As noted above, an independent approach by Ward et al. (2019) resulted in similar estimate for the flux of recycled P toward the end of the Archean, supporting a lower recycling efficiency of P than the modern value (~0.997).

Recently, Kipp and Stueken (2017) compiled the availability of oxidants for recycling P through Earth history and used these to argue that rates of P recycling in Archean seawater were 100 times lower than the modern, i.e., a recycling efficiency < 0.01. Kipp & Stueken's estimate should represent a lower limit of recycling efficiency, considering the preferential release of P during organic decomposition (Clark et al., 1998) and photo-oxidation of organics in surface seawater (see below). Moreover the absence of zooplankton and fecal pellets in the Archean ocean might have led to less efficient deposition of particulate organic carbon (Logan et al., 1995) and, consequently, burial of organic matter in the Archean ocean.

It is also important to ask whether the recycling efficiency of nutrients might have evolved through Archean time as a function of the redox state of surface environments (Hao et al., 2019) and continental emergence (thus, shelf area for upwelling; see Olson et al., 2019). In the early Archean, when surface environments were more reducing and emergent continents were minimal, recycling of organic matter would be severely depressed due to oxidant limitation and limited shelf area for upwelling (Fig. 8a). However, in the middle to late Archean, oxidant inventories increased (Stueken et al., 2012) and continental lands increasingly emerged above sea level (Flament et al., 2013; Korenaga et al., 2017). Back reduction of river-transported sulfate might have depleted dissolved seawater Fe(II) regionally, even generating euxinic areas in the late Archean ocean (Reinhard et al., 2009). The solubility of vivianite would increase significantly in regionally euxinic zones, engendering a simultaneous increase of P solubility (Fig. 8b). As a consequence, the recycling efficiency of nutrients would be expected to increase.

In modern surface seawater, dissolved organic P (DOP) can reach significant levels, sometimes even higher than dissolved inorganic P (Ruttenberg. 2014). Due to the high stability of biomolecules under reducing conditions, organic P might have also been important in the Archean seawater. However, experimental studies have suggested that the lifetime of organic-P under UV radiation would be short (Francko and Heath, 1979). Thus, high UV radiation, due to the lack of an Archean ozone shield, might efficiently destroy organic P in the surface layers of Archean seawater. Therefore, dissolved organic P might have played a relatively minor role for the Archean life in photic zone.

4.5. Electron vs. phosphorus limitation on Archean primary production?

How do the simulations presented here inform the debate about nutrient versus electron donor limitation on net primary production (NPP) in Archean oceans? Total fluxes of electron donors on the Archean Earth have been proposed in several studies (Kharecha et al., 2005; Canfield et al., 2006; Ward et al., 2019), but estimated values vary markedly (Fig. 9). By comparison, fluxes of nutrients have been less commonly investigated (Laakso and Schrag, 2018; Ward et al., 2019), particularly for phosphorus, thought to be the most probable limiting nutrient.

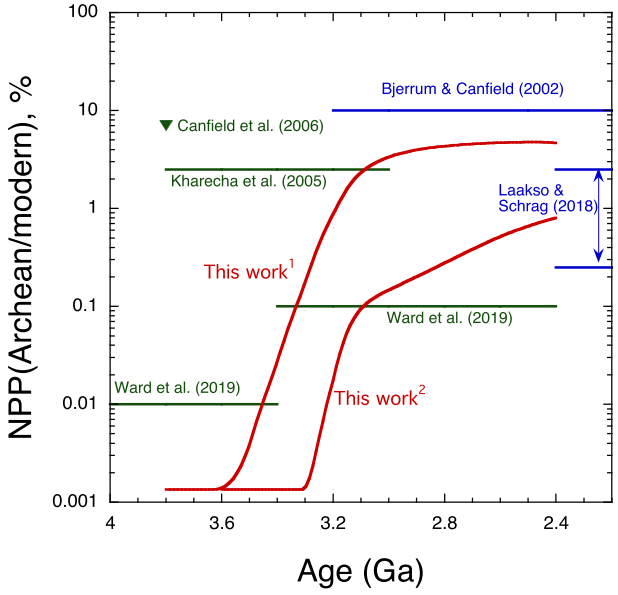

Fig. 9. Upper limits of net primary production (NPP) in the ocean through the Archean Eon relative to the modern level. Blue lines show the previously reported constraints (upper limit or range) of NPP by the supply of P (Bjerrum and Canfield, 2002; Laakso and Schrag, 2018). Green lines display the previously reported constraints (upper limits) of NPP by the supply of electron donors (Canfield et al., 2006; Kharecha et al., 2005; Ward et al., 2019) and efficiency of early metabolisms (Ward et al., 2019). Red curves present our reconstructed evolution (upper limits) of NPP limited by the supply of P assuming: (1) slow emergence of land in the late Archean (Flament et al., 2013); (2) rapid emergence of land in the late Archean (Korenaga et al, 2017).

[It has been proposed that nitrogen limits global primary production on geologic time scales (Falkowski, 1997), but at the low levels for Archean NPP advocated here, nitrogen demand could have been met by modest rates of biological nitrogen fixation, and, especially during the early Archean, might have been sustained in most times and in many places by abiotic N-fixation (Chameides and Walker, 1981; Wong et al., 2017; Ward et al., 2019).]

Various lines of evidence support the concept of a more or less low-P Archean ocean (Bjerrum and Canfield, 2002; Planavsky et al., 2010; Jones et al., 2015; Reinhard et al., 2017). Here, we estimate that the total flux of P could have reached 18–154 $\times 10^{10}$ moles P/yr by the end of the Archean Eon. Assuming a standard Redfield C:P of 106:1, this is equivalent to a NPP of 19–163 $\times 10^{12}$ moles C/yr, or 0.5–4% of the modern value (ca. 4000 $\times 10^{12}$ moles C/yr; Field et al., 1998). In the modern ocean, Redfield ratios of individual populations vary within limits set by the fundamental biochemical composition of their constituent cells (Geider and La Roche, 2002). If, following Laakso and Schrag (2018), we accept that mean C:P could have reached values as high at 195:1, the total flux of P could have supported up to 7% of the modern NPP by the end of the Archean Eon. This level of NPP is higher than the estimate by Ward et al. (2019), i.e. <0.1% for the late Archean time limited by the availability of electron donors and the efficiency of anoxygenic photosynthesis.

We stress, however, that our estimated P flux varies markedly through a billion years of recorded Archean history (Hao et al., 2020; Fig. 9. Early in the Archean, when continental weathering of P was severely limited by continental exposure and elevation, the weathering and erosional flux of P from continents would have been extremely low (Table 1). Because of this factor and limitations on recycling efficiency from both low oxidant supply and the probability of P capture by vivianite, P supplied by recycling would also have been extremely low (Table 1 & Fig. 8a). Moreover, the limited area of emergent continents and, thus, coastal continental margin shelf could result in relatively weak upwelling, and in consequence, reduced nutrient recycling (Olson et al., 2019). P, then, could have limited NPP to less than 0.05 $\times 10^{12}$ moles C/yr, a factor of eight lower than Ward et al.'s estimate for an Archean biosphere fueled by anoxygenic photosynthesis and far lower than the value estimated by Canfield et al. (2006). Altogether, these results might indicate transition from a P-limited biosphere in the early Archean to an electron donor-limited biosphere as continents emerged toward the end of Archean (Fig. 9).

Questions of NPP limitation by P or electron donors are straightforward only in a world without oxygenic photosynthesis. Once bacteria evolved the capacity to split water, the supply of electron donors became essentially unlimited and primary production would, forever after, be limited by nutrient availability, primarily phosphorus (Tyrrell, 1999). Despite continuing debate about when oxygenic photosynthesis first evolved, there is a consensus that the oxygenation of atmosphere at 2.4 Ga required oxygenic photosynthesis. Ward et al. (2016) simulated the oxygenation time of the Archean atmosphere under a series of settings (primary production, burial fraction, and methanogenic fraction) and suggested that with a primary production of 10^{14} moles C/yr, irreversible oxygenation of atmosphere would happen within ~100 kyr. This level of primary production falls into the range of NPP supported by our estimation of total P in the end of Archean Eon (Table 1). Therefore, increasing emergence of continents and riverine transport of phosphorus would lead to higher primary productivity and once oxygenic autotrophs attained ecological prominence, rapid oxygenation of atmosphere as the Proterozoic Eon began.

5. CONCLUSIONS

The total flux of P for marine ecosystems predominantly reflects input from continental weathering and the recycling of P within the ocean. Archean seawater was anoxic, with a limited supply of oxidants, suppressing P recycling and so linking primary production more closely to continental weathering. Although Archean seawater was weakly acidic, apatite solubility would have been very low due to high levels of Ca and halogens; for this reason, seafloor weathering of P should not have been a major source of P for Archean marine ecosystems. In addition, the solubility of vivianite is predicted to have remained very low (0.1–0.3 μM) at moderate supersaturation states (Q/K = 100–1000) in Archean ferruginous seawater. Under these conditions, the precipitation flux of vivianite could have reached a level comparable to or higher than the modern sinking flux for P; therefore, it might have been a major sink in the Archean P cycle, with precipitation kinetically facilitated by microbial metabolism and mineral adsorption. Although potentially delivered to accumulating sediments, vivianite would not have been stable during burial diagenesis and metamorphism, reacting readily with calcium carbonate to form more stably calcium phosphates, particularly apatite.

Together with continental input of P, our current estimate of recycling P in the Archean ocean would, under the most favorable circumstances, have allowed up to 7% of modern NPP by the end of the Archean Eon. However, during the early and middle Archean, inputs of continental weathering and P recycling would have been considerably weaker, and the fluxes of electron donors higher. Therefore, NPP of the Archean marine ecosystems may well have been limited by the availability of P instead of electron donors during most of the Archean Eon. Indeed, on the early Archean Earth, NPP may well have been too low to oxygenate the atmosphere and surface ocean, even if oxygenic photoautotrophs were widely distributed in marine and fresh waters. Therefore, rapid oxygenation of the atmosphere might only have become possible as increasing P fluxes from weathering and erosion increased near the end of Archean Eon.

Declaration of Competing Interest

The authors declare that they have no known competing financial interests or personal relationships that could have appeared to influence the work reported in this paper.

ACKNOWLEDGEMENTS

We thank Dimitri A. Sverjensky, Cin-Ty Lee, Nicolas Coltice, Ciaran Harman, Mathew Pasek, Michael Kipp, David Catling, Lu Pan, Chao Liu, Liyan Tian, Ming Tang, Joshua Krissansen-Totton, Dustin Trail, and Paul Falkowski for helpful discussions. We also appreciate constructive comments by three anonymous reviewers, Nicolas Tosca, and Jeffrey Catalano. JHH & ID thank French National Research Agency (#ANR-15-CE31-0010), JHH & RMH thank NASA's Astrobiology Institute grant (80NSSC18M0093), and JHH, AHK, FH, and RMH thank W.M. Keck Foundation for financial support. RMH thanks the Templeton Foundation for financial support. JS thanks the sponsors of the Indiana University Shale Research Consortium (Anadarko, Chevron, ConocoPhillips, ExxonMobil, Shell, Equinor, Marathon, Whiting, and Wintershall) for support of the IU Shale Research Lab.

AUTHOR CONTRIBUTIONS

JHH and AHK conceived of the project. JHH and FH performed the simulations; JHH and AHK analyzed the results. JS and AHK collected and investigated the textural mode of apatite grains in Archean and Proterozoic shales. All authors discussed the results and wrote the manuscript.

RESEARCH DATA

Thermodynamic properties of chemical reactions are provided in supplementary file. The continental weathering and seawater chemistry models are calculated using the codes shared online by Krissansen-Totton (https://github.com/joshuakt/early-earth-carbon-cycle) with additional modifications on continental emergence (see main text).

REFERENCES

Al-Borno A. and Tomson M. B. (1994) The temperature dependence of the solubility product constant of vivianite. *Geochim. Cosmochim. Acta* **58**, 5373–5378.

Alt J. C. and Honnorez J. (1984) Alteration of the upper oceanic crust, DSDP site 417: mineralogy and chemistry. *Contrib. Mineral. Petr.* **87**, 149–169.

Anbar A. D., Duan Y., Lyons T. W., Arnold G. L., Kendall B., Creaser R. A., Kaufman A. J., Gordon G. W., Scott C., Garvin J. and Buick R. (2007) A whiff of oxygen before the great oxidation event? *Science (80-.)* **317**, 1903–1906.

Anderson A. T. and Greenland L. P. (1969) Phosphorus fractionation diagram as a quantitative indicator of crystallization differentiation of basaltic liquids. *Geochim. Cosmochim. Acta* **33**, 493–505.

Baturin G. (2003) Phosphorus cycle in the ocean. *Lithol. Miner. Resour.* **38**, 101–119.

Bindeman I. N., Zakharov D. O., Palandri J., Greber N. D., Dauphas N., Retallack G. J., Hofmann A., Lackey J. S. and Bekker A. (2018) Rapid emergence of subaerial landmasses and onset of a modern hydrologic cycle 2.5 billion years ago. *Nature* **557**, 545–548.

Bjerrum C. J. and Canfield D. E. (2002) Ocean productivity before about 1.9 Gyr ago limited by phosphorus adsorption onto iron oxides. *Nature* **417**, 159–162.

Borch T. and Fendorf S. (2007) *Chapter 12 phosphate interactions with iron (hydr)oxides: mineralization pathways and phosphorus retention upon bioreduction*. Elsevier, pp. 321–348.

Brantley S. L. and Olsen A. A. (2014) Reaction kinetics of primary rock-forming minerals under ambient conditions. In *Treatise on Geochemistry* (eds. H. D. Holland and K. K. Turekian), second edition. Elsevier, Oxford, pp. 69–113.

Brunet F. and Chazot G. (2001) Partitioning of phosphorus between olivine, clinopyroxene and silicate glass in an spinel lherzolite xenolith from Yemen. *Chem. Geol.* **176**, 51–72.

Byrne R. H. and Kim K. H. (1993) Rare earth precipitation and coprecipitation behavior: The limiting role of PO43- on dissolved rare earth concentrations in seawater. *Geochim. Cosmochim. Acta* **57**, 519–526.

Canfield D. E., Rosing M. T. and Bjerrum C. (2006) Early anaerobic metabolisms. *Philos. Trans. R. Soc. B Biol. Sci.* **361**, 1819–1834.

Cardona T., Sánchez-Baracaldo P., Rutherford A. W. and Larkum A. W. (2019) Early Archean origin of photosystem II. *Geobiology* **17**, 127–150.

Chameides W. L. and Walker J. C. G. (1981) Rates of fixation by lightning of carbon and nitrogen in possible primitive atmospheres. *Orig. Life* **11**, 291–302.

Clark L. L., Ingall E. D. and Benner R. (1998) Marine phosphorus is selectively remineralized. *Nature* **393**, 426.

Compton J., Mallinson D., Glenn C. R., Filippelli G., Follmi K., Shields G. and Zanin Y. (2010) Variations in the global phosphorus cycle. *Mar. Authigenes. From Glob. to Microb.*, 21–33.

Coogan L. A., MacLeod C. J., Dick H. J. B., Edwards S. J., Kvassnes A., Natland J. H., Robinson P. T., Thompson G. and O'Hara M. J. (2001) Whole-rock geochemistry of gabbros from the Southwest Indian Ridge: Constraints on geochemical fractionations between the upper and lower oceanic crust and magma chamber processes at (very) slow-spreading ridges. *Chem. Geol.* **178**, 1–22.

Cosmidis J., Benzerara K., Morin G., Busigny V., Lebeau O., Jézéquel D., Noël V., Dublet G. and Othmane G. (2014) Biomineralization of iron-phosphates in the water column of Lake Pavin (Massif Central, France). *Geochim. Cosmochim. Acta* **126**, 78–96.

Crowe S. A., Katsev S., Leslie K., Sturm A., Magen C., Nomosatryo S., Pack M. A., Kessler J. D., Reeburgh W. S., Roberts J. A., González L., Douglas Haffner G., Mucci A., Sundby B. and Fowle D. A. (2011) The methane cycle in ferruginous Lake Matano. *Geobiology* **9**, 61–78.

de Kanel J. and Morse J. W. (1978) The chemistry of orthophosphate uptake from seawater on to calcite and aragonite. *Geochim. Cosmochim. Acta* **42**, 1335–1340.

Derry L. A. (2015) Causes and consequences of mid-Proterozoic anoxia. *Geophys. Res. Lett.* **42**, 8538–8546.

Eanes E. D. and Meyer J. L. (1977) The maturation of crystalline calcium phosphates in aqueous suspensions at physiologic pH. *Calcif. Tissue Res.* **23**, 259–269.

Falkowski P. G. (1997) Evolution of the nitrogen cycle and its influence on the biological sequestration of CO2 in the ocean. *Nature* **387**, 272–275.

Field C. B. (eld) Primary production of the biosphere: integrating terrestrial and oceanic components. *Science (80-.)* **281**, 237–240. https://doi.org/10.1126/science:281.5374.237.

Fischer W. W., Hemp J. and Johnson J. E. (2016) Evolution of oxygenic photosynthesis. *Annu. Rev. Earth Planet. Sci.* **44**, 647–683.

Flament N., Coltice N. and Rey P. F. (2013) The evolution of the87Sr/86Sr of marine carbonates does not constrain continental growth. *Precambrian Res.* **229**, 177–188.

Fourqurean J. W., Zieman J. C. and Powell G. V. N. (1992) Phosphorus limitation of primary production in Florida Bay: Evidence from C:N: P ratios of the dominant seagrass Thalassia testudinum. *Limnol. Oceanogr.* **37**, 162–171.

Francko D. A. and Heath R. T. (1979) Functionally distinct classes of complex phosphorus compounds in lake water. *Limnol. Oceanogr.* **24**, 463–473.

Freeman J. S. and Rowell D. L. (1981) The adsorption and precipitation of phosphate onto calcite. *J. Soil Sci.* **32**, 75–84.

Friend C. R. L., Nutman A. P., Bennett V. C. and Norman M. D. (2008) Seawater-like trace element signatures (REE + Y) of Eoarchaean chemical sedimentary rocks from southern West Greenland, and their corruption during high-grade metamorphism. *Contrib. Mineral. Petrol.* **155**, 229–246.

Geider R. J. and La Roche J. (2002) Redfield revisited: Variability of C:N: P in marine microalgae and its biochemical basis. *Eur. J. Phycol.* **37**, 1–17.

Green T. H. and Watson E. B. (1982) Crystallization of apatite in natural magmas under high pressure, hydrous conditions, with particular reference to "Orogenic" rock series. *Contrib. Mineral. Petrol.* **79**, 96–105.

Guidry M. W. and Mackenzie F. T. (2003) Experimental study of igneous and sedimentary apatite dissolution. *Geochim. Cosmochim. Acta* **67**, 2949–2963.

Gunnars A., Blomqvist S. and Martinsson C. (2004) Inorganic formation of apatite in brackish seawater from the Baltic Sea: An experimental approach. *Mar. Chem.* **91**, 15–26.

Halevy I. and Bachan A. (2017) The geologic history of seawater pH. *Science (80-.)* **355**, 1069–1071.

Halevy I., Alesker M., Schuster E. M., Popovitz-Biro R. and Feldman Y. (2017) A key role for green rust in the Precambrian oceans and the genesis of iron formations. Nat. Geosci.10, 135. Available at: https://doi.org/10.1038/ngeo2878

Hansen B. C. H. and Poulsen I. F. (1999) Interaction of synthetic sulphate green rust with phosphate and the crystallization of vivianite. *Clays Clay Miner.* **47**, 312–318.

Hao J., Sverjensky D. A. and Hazen R. M. (2017) Mobility of nutrients and trace metals during weathering in the late Archean. *Earth Planet. Sci. Lett.* **471**, 148–159.

Hao J., Sverjensky D. A. and Hazen R. M. (2019) Redox states of Archean surficial environments: The importance of H2, g instead of O2, g for weathering reactions. *Chem. Geol.* **521**, 49–58.

Hao J., Knoll A. H., Huang F., Hazen R. M. and Daniel I. (2020) Cycling phosphorus on the archean earth: Part I. Continental weathering and riverine transport of phosphorus. *Geochim. Cosmochim. Acta* **273**, 70–84.

Hartnett H. E., Keil R. G., Hedges J. I. and Devol A. H. (1998) Influence of oxygen exposure time on organic carbon preservation in continental margin sediments. *Nature* **391**, 572–574.

Hawkesworth C. J., Cawood P. A., Dhuime B. and Kemp T. I. S. (2017) Earth's continental lithosphere through time. *Annu. Rev. Earth Planet. Sci.* **45**, 169–198.

Hedges J. I., Hu F. S., Devol A. H., Hartnett H. E., Tsamakis E. and Keil R. G. (1999) Sedimentary organic matter preservation: A test for selective degradation under oxic conditions. *Am. J. Sci.* **299**, 529–555.

Hedges J. I. and Keil R. G. (1995) Sedimentary organic matter preservation: an assessment and speculative synthesis. *Mar. Chem.* **49**, 81–115.

Herschy B., Chang S. J., Blake R., Lepland A., Abbott-Lyon H., Sampson J., Atlas Z., Kee T. P. and Pasek M. A. (2018) Archean phosphorus liberation induced by iron redox geochemistry. *Nat. Commun.*, 9.

Isson T. T. and Planavsky N. J. (2018) Reverse weathering as a long-term stabilizer of marine pH and planetary climate. *Nature* **560**, 471–475.

Jiang C. Z. and Tosca N. J. (2019) Fe(II)-carbonate precipitation kinetics and the chemistry of anoxic ferruginous seawater. *Earth Planet. Sci. Lett.* **506**, 231–242.

Jilbert T. and Slomp C. P. (2013) Iron and manganese shuttles control the formation of authigenic phosphorus minerals in the euxinic basins of the Baltic Sea. *Geochim. Cosmochim. Acta* **107**, 155–169.

Johnson B. R., Tostevin R., Gopon P., Wells J., Robinson S. A. and Tosca N. J. (2020) Phosphorus burial in ferruginous SiO2-rich Mesoproterozoic sediments. *Geology* **48**, 92–96.

Johnson J. E., Muhling J. R., Cosmidis J., Rasmussen B. and Templeton A. S. (2018) Low-Fe(III) greenalite was a primary mineral from neoarchean oceans. *Geophys. Res. Lett.* **45**, 3182–3192.

Johnson J. W., Oelkers E. H. and Helgeson H. C. (1992) SUPCRT92: A software package for calculating the standard molal thermodynamic properties of minerals, gases, aqueous species, and reactions from 1 to 5000 bar and 0 to 1000°C. *Comput. Geosci.* **18**, 899–947.

Jones C., Nomosatryo S., Crowe S. A., Bjerrum C. J. and Canfield D. E. (2015) Iron oxides, divalent cations, silica, and the early earth phosphorus crisis. *Geology* **43**, 135–138.

Kakegawa T. (2003) Establishment of the phosphorous cycle in early Archean oceans. *Geochim. Cosmochim. Acta Suppl.* **67**, 194.

Katsev S. and Crowe S. A. (2015) Organic carbon burial efficiencies in sediments: The power law of mineralization revisited. *Geology* **43**, 607–610.

Kaufman A. J., Johnston D. T., Farquhar J., Masterson A. L., Lyons T. W., Bates S., Anbar A. D., Arnold G. L., Garvin J. and Buick R. (2007) Late archean biospheric oxygenation and atmospheric evolution. *Science (80-.)* **317**, 1900–1903.

Kharecha P., Kasting J. and Siefert J. (2005) A coupled atmosphere-ecosystem model of the early Archean earth. *Geobiology* **3**, 53–76.

Kipp M. A. (2019) Causes and consequences of high burial efficiency in the Archean ocean. In: 2nd Geobiology Society Conference.

Kipp M. A. and Stüeken E. E. (2017) Biomass recycling and Earth's early phosphorus cycle. *Sci. Adv.*, 3.

Konhauser K. O., Lalonde S. V., Amskold L. and Holland H. D. (2007) Was there really an Archean phosphate crisis? *Science (80-.)* **315**, 1234.

Kopp R. E., Kirschvink J. L., Hilburn I. A. and Nash C. Z. (2005) The Paleoproterozoic snowball Earth: A climate disaster triggered by the evolution of oxygenic photosynthesis. *Proc. Natl. Acad. Sci.* **102**, 11131–11136.

Korenaga J., Planavsky N. J. and Evans D. A. D. (2017) Global water cycle and the coevolution of the Earth's interior and surface environment. *Philos. Trans. R. Soc. A Math. Phys. Eng. Sci.*, 375.

Kraal P., Dijkstra N., Behrends T. and Slomp C. P. (2017) Phosphorus burial in sediments of the sulfidic deep Black Sea: Key roles for adsorption by calcium carbonate and apatite authigenesis. *Geochim. Cosmochim. Acta* **204**, 140–158.

Krajewski K. P., Cappellen P. va, Trichet J., Kuhn O., LuCAs J., Martín-Algarra A., Prevot L., Tewari V. C., Gaspar L. and Knight R. I. (1994) Biological processes and apatite formation in sedimentary environments. *Eclogae Geol. Helv.* **87**, 701–746.

Krissansen-Totton J., Arney G. N. and Catling D. C. (2018) Constraining the climate and ocean pH of the early Earth with a geological carbon cycle model. *Proc. Natl. Acad. Sci.*, 201721296.

Kuntz L. B., Laakso T. A., Schrag D. P. and Crowe S. A. (2015) Modeling the carbon cycle in Lake Matano. *Geobiology* **13**, 454–461.

Laakso T. A. and Schrag D. P. (2018) Limitations on limitation. *Global Biogeochem. Cycles* **32**, 486–496.

Lenstra W. K., Egger M., van Helmond N. A. G. M., Kritzberg E., Conley D. J. and Slomp C. P. (2018) Large variations in iron input to an oligotrophic Baltic Sea estuary: impact on sedimentary phosphorus burial. *Biogeosci. Discuss.* **15**, 6979–6996.

Lepland A., Arrhenius G. and Cornell D. (2002) Apatite in early Archean Isua supracrustal rocks, southern West Greenland: Its origin, association with graphite and potential as a biomarker. *Precambrian Res.* **118**, 221–241.

Liu J., Cheng X., Qi X., Li N., Tian J., Qiu B., Xu K. and Qu D. (2018) Recovery of phosphate from aqueous solutions via vivianite crystallization: Thermodynamics and influence of pH. *Chem. Eng. J.* **349**, 37–46.

Logan G. A., Hayes J. M., Hieshima G. B. and Summons R. E. (1995) Terminal Proterozoic reorganization of biogeochemical cycles. *Nature* **376**, 53–56.

Lyons T. W. and Gill B. C. (2010) Ancient sulfur cycling and oxygenation of the early biosphere. *Elements* **6**, 93–99.

Madsen H. E. L. (2019) Influence of calcium and aluminum on crystallization of vivianite, Fe3(PO4)2·8H2O. *J. Cryst. Growth* **526**, 125242.

Madsen H. E. L. and Hansen H. C. B. (2014) Kinetics of crystal growth of vivianite, Fe3(PO4)2·8H2O, from solution at 25, 35 and 45 °C. *J. Cryst. Growth* **401**, 82–86.

Marty B., Avice G., Bekaert D. V. and Broadley M. W. (2018) Salinity of the Archaean oceans from analysis of fluid inclusions in quartz. *Comptes Rendus - Geosci.* **350**, 154–163.

Meurer W. P. and Natland J. H. (2001) Apatite compositions from oceanic cumulates with implications for the evolution of mid-ocean ridge magmatic systems. *J. Volcanol. Geotherm. Res.* **110**, 281–298.

Millero F., Huang F., Zhu X., Liu X. and Zhang J. Z. (2001) Adsorption and desorption of phosphate on calcite and aragonite in seawater. *Aquat. Geochem.* **7**, 33–56.

Murakami A., Sawaki Y., Ueda H., Orihashi Y., Machida S., and Komiya T. (2019) Behavior of phosphorus during hydrothermal alteration of basalt under CO2-rich condition. In: Japan Geoscience Union Meeting 2019.

Nancollas G. H. (1984) The nucleation and growth of phosphate minerals. In *Phosphate Minerals* (eds. J. O. Nriagu and P. B. Moore). Springer, Berlin Heidelberg, Berlin, Heidelberg, pp. 137–154.

Olson S. L., Jansen M. and Abbot D. S. (2019) Oceanographic constraints on exoplanet life. arXiv Prepr. arXiv1909.02928.

Oxmann J. F. and Schwendenmann L. (2015) Authigenic apatite and octacalcium phosphate formation due to adsorption–precipitation switching across estuarine salinity gradients. *Biogeosciences* **12**, 723–738.

Paytan A. and McLaughlin K. (2007) The oceanic phosphorus cycle. *Chem. Rev.* **107**, 563–576.

Planavsky N. J., Rouxel O. J., Bekker A., Lalonde S. V., Konhauser K. O., Reinhard C. T. and Lyons T. W. (2010) The evolution of the marine phosphate reservoir. *Nature* **467**, 1088–1090.

Rasmussen B. (2000) The impact of early-diagenetic aluminophosphate precipitation on the oceanic phosphorus budget. *Mar. Authigenes. From Glob. Microb.*, 89–101.

Rasmussen B., Muhling J. R., Suvorova A. and Krapež B. (2016) Dust to dust: Evidence for the formation of "primary" hematite dust in banded iron formations via oxidation of iron silicate nanoparticles. *Precambrian Res.* **284**, 49–63.

Reinhard C. T., Planavsky N. J., Gill B. C., Ozaki K., Robbins L. J., Lyons T. W., Fischer W. W., Wang C., Cole D. B. and Konhauser K. O. (2017) Evolution of the global phosphorus cycle. *Nature* **541**, 386–389.

Reinhard C. T., Raiswell R., Scott C., Anbar A. D. and Lyons T. W. (2009) A late archean sulfidic sea stimulated by early oxidative weathering of the continents. *Science (80-.)* **326**, 713–716.

Rothe Matthia, Kleeberg Andrea, Grüneberg Björ, Friese Kur, Pérez-Mayo Manue, Hupfer Michae and Boyanov Maxim I. (2015) Sedimentary sulphur:iron ratio indicates vivianite occurrence: a study from two contrasting freshwater systems. *PLoS ONE* **10**.

Rothe M., Kleeberg A. and Hupfer M. (2016) The occurrence, identification and environmental relevance of vivianite in waterlogged soils and aquatic sediments. *Earth-Sci. Rev.* **158**, 51–64.

Rubinstein N., Fazio A. M., Scasso R. A. and Carey S. (2013) Association of phosphate with rhyolite glass in marine Neogene tuffs from Patagonia, Argentina. *Sedimentology* **60**, 1007–1016.

Ruttenberg K. C. (2014) The global phosphorus cycle. In *Treatise on Geochemistry: Second Edition* (eds. H. D. Holland and K. K. Turekian). Elsevier, Oxford, pp. 499–558.

Sánchez-Román M., Puente-Sánchez F., Parro V. and Amils R. (2015) Nucleation of Fe-rich phosphates and carbonates on microbial cells and exopolymeric substances. *Front. Microbiol.*, 6.

Schieber J., Sur S. and Banerjee S. (2007) Benthic microbial mats in black shale units from the Vindhyan Supergroup, Middle Proterozoic of India: the challenges of recognizing the genuine article. Atlas Microb. mat Featur. Preserv. within clastic rock Rec. Amsterdam, Elsevier, pp. 189–197.

Schlesinger W. H. and Bernhardt E. S. (2013) *Biogeochemistry: An Analysis of Global Change*. Academic Press.

Schneiderhan E., Zimmermann U., Gutzmer J., Mezger K. and Armstrong R. (2011) Sedimentary provenance of the neoarchean ventersdorp supergroup, Southern Africa: Shedding light on the evolution of the kaapvaal craton during the neoarchean. *J. Geol.* **119**, 575–596.

Siever R. (1992) The silica cycle in the Precambrian. *Geochim. Cosmochim. Acta* **56**, 3265–3272.

Sleep N. H. and Zahnle K. (2001) Carbon dioxide cycling and implications for climate on ancient Earth. *J. Geophys. Res.* **106**, 1373.

Staudigel H., Furnes H., McLoughlin N., Banerjee N. R., Connell L. B. and Templeton A. (2008) 3.5 billion years of glass bioalteration: Volcanic rocks as a basis for microbial life? *Earth-Sci. Rev.* **89**, 156–176.

Stüeken E. E., Catling D. C. and Buick R. (2012) Contributions to late Archaean sulphur cycling by life on land. *Nat. Geosci.* **5**, 722–725.

Syverson D. D., Reinhard C. T., Isson T. T., Holstege C., Katchinoff J., Tutolo B. M., Etschmann B., Brugger J. and Planavsky N. J. (2020) Anoxic weathering of mafic oceanic crust promotes atmospheric oxygenation. arXiv Prepr. arXiv2002.07667.

Thinnappan V., Merrifield C. M., Islam F. S., Polya D. A., Wincott P. and Wogelius R. A. (2008) A combined experimental study of vivianite and As (V) reactivity in the pH range 2–11. *Appl. Geochem.* **23**, 3187–3204.

Tosca N. J., Guggenheim S. and Pufahl P. K. (2016) An authigenic origin for Precambrian greenalite: Implications for iron forma-

tion and the chemistry of ancient seawater. *Bull. Geol. Soc. Am.* **128**, 511–530.

Tosca N. J., Jiang C. Z., Rasmussen B. and Muhling J. (2019) Products of the iron cycle on the early Earth. *Free Radic. Biol. Med.*. https://doi.org/10.1016/j.freeradbiomed.2019.05.005, in press.

Tréguer P. J. and De La Rocha C. L. (2012) The world ocean silica cycle. *Ann. Rev. Mar. Sci.* **5**, 477–501.

Tsukamoto Y., Kakegawa T., Graham U., Liu Z.-K., Ito A. and Ohmoto H. (2018) Discovery of Ni-Fe phosphides in the 3.46 Ga-old apex basalt: implications on the phosphate budget of the Archean oceans. *Goldschmidt Abstr.*.

Tyrrell T. (1999) The relative influences of nitrogen and phosphorus on oceanic primary production. *Nature* **400**, 525–531.

Van Cappellen P. S. and Berner R. A. (1991) *The Formation of Marine Apatite: A Kinetic Study*. Yale University.

Vuillemin A., Wirth R., Kemnitz H., Schleicher A. M., Friese A., Bauer K. W., Simister R., Nomosatryo S., Ordoñez L., Ariztegui D., Henny C., Crowe S. A., Benning L. G., Kallmeyer J., Russell J. M., Bijaksana S., Vogel H. and Team the T. D. P. S. (2019) Formation of diagenetic siderite in modern ferruginous sediments. *Geology* **47**, 540–544.

Walpersdorf E., Koch C. B., Heiberg L., O'Connell D. W., Kjaergaard C. and Hansen H. C. B. (2013) Does vivianite control phosphate solubility in anoxic meadow soils? *Geoderma* **193–194**, 189–199.

Ward L. M., Kirschvink J. L. and Fischer W. W. (2016) Timescales of oxygenation following the evolution of oxygenic photosynthesis. *Orig. Life Evol. Biosph.* **46**, 51–65.

Ward L. M., Rasmussen B. and Fischer W. W. (2019) Primary productivity was limited by electron donors prior to the advent of oxygenic photosynthesis. *J. Geophys. Res. Biogeosci.* **124**, 211–226.

Wheat C. G., Feely R. A. and Mottl M. J. (1996) Phosphate removal by oceanic hydrothermal processes: An update of the phosphorus budget in the oceans. *Geochim. Cosmochim. Acta* **60**, 3593–3608.

Wong M. L., Charnay B. D., Gao P., Yung Y. L. and Russell M. J. (2017) Nitrogen oxides in early earth's atmosphere as electron acceptors for life's emergence. *Astrobiology* **17**, 975–983.

Xiong Y. (2019) *Phosphorus Cycling Under Different Redox Conditions*. University of Leeds.

Xu N., Chen M., Zhou K., Wang Y., Yin H. and Chen Z. (2014) Retention of phosphorus on calcite and dolomite: speciation and modeling. *RSC Adv.* **4**, 35205–35214.

Zegeye A., Bonneville S., Benning L. G., Sturm A., Fowle D. A., Jones C. A., Canfield D. E., Ruby C., MacLean L. C., Nomosatryo S., Crowe S. A. and Poulton S. W. (2012) Green rust formation controls nutrient availability in a ferruginous water column. *Geology* **40**, 599–602.

Zonneveld K. A. F., Versteegh G. J. M., Kasten S., Eglinton T. I., Emeis K. C., Huguet C., Koch B. P., De Lange G. J., De Leeuw J. W., Middelburg J. J., Mollenhauer G., Prahl F. G., Rethemeyer J. and Wakeham S. G. (2010) Selective preservation of organic matter in marine environments; Processes and impact on the sedimentary record. *Biogeosciences* **7**, 483–511.

Associate editor: Nicholas Tosca